Atmos. Chem. Phys. Discuss., 3, 4833–4856, 2003
www.atmos-chem-phys.org/acpd/3/4833/

Atmospheric Chemistry and Physics Discussions

Ground-based water vapour soundings by microwave radiometry and Raman lidar on Jungfraujoch (Swiss Alps)

D. Gerber[1], I. Balin[2], D. Feist[1], N. Kämpfer[1], V. Simeonov[2], B. Calpini[2,*], and H. van den Bergh[2]

[1]Institute of Applied Physics, University of Bern, Switzerland
[2]Laboratory of Air Pollution, Swiss Federal Institute of Technology – Lausanne (EPFL), Lausanne, Switzerland
[*]Now at: MétéoSuisse, Payerne Station, Switzerland

Received: 23 June 2003 – Accepted: 2 September 2003 – Published: 25 September 2003

Correspondence to: D. Gerber (daniel.gerber@mw.iap.unibe.ch)

Abstract

Water vapour has been measured from the International Scientific Station Jungfraujoch (ISSJ, 47° N, 7° E, 3580 m a.s.l.) during the winters of 1999/2000 and 2000/2001 by microwave radiometry and Raman lidar. The abundance of atmospheric water vapour between the planetary boundary layer and the upper stratosphere varies over more than three orders of magnitude. The currently used measurement techniques are suited to determine the abundance of water vapour in different atmospheric regimes, however none can resolve by itself a vertical distribution profile over a full altitude range from ground level to the top of the stratosphere. We present such a water vapour profile where simultaneous measurements from a Raman lidar and a microwave radiometer are combined to cover both the troposphere and the stratosphere, respectively. We also present a study of the stratospheric and tropospheric water vapour variability for the two consecutive winters.

1. Introduction

The distribution of water vapour in the Earth's atmosphere is regaining the interest of the scientific community in the recent past (Kley et al., 2000; Starr and Melfie, 1991). With the arising of new questions concerning the trend in water vapour (Nedoluha et al., 1998), exchange processes across the tropopause and the impact on radiative forcing as well directly (water vapour is the most important greenhouse gas) as indirectly through the formation of clouds, the need for water vapour measurements has increased lately. However, the large gradient of more than three orders of magnitude in abundance between the planetary boundary layer and the stratosphere is a serious challenge for each measuring technique and every technique, be it ground- or satellite-based remote sensing or in situ sampling of air parcels is generally limited to a certain altitude range where it produces its best results (Starr and Melfie, 1991; England et al., 1992). We present in this work a profile of atmospheric water vapour which reaches

from the earth's surface to the upper stratosphere at 60 km. The profile is a combined sampling of the air column above the ISSJ by simultaneous measurements of tropospheric water vapour by a Raman lidar and of stratospheric water vapour by a microwave radiometer.

2. Measurement techniques

2.1. Microwave radiometry

In passive microwave radiometry of molecules the electromagnetic emission from transitions between different states of rotational energy are measured by a receiver. The linewidth of the observed spectral emission line is affected by different broadening processes. In the altitude range up to the stratopause and sometimes even up into the mesosphere the dominating process is pressure broadening, the forced microwave emission by pressure-induced collisions. Because of the known relation between pressure and altitude, pressure broadening introduces altitude dependent information to the total spectral emission observed at ground level. From the spectrum observed at ground level the contributions from each altitude layer can afterwards be retrieved by inverse methods. We use an optimal estimation approach with an *a priori* profile as set forth by Rodgers (2000) to derive a vertical abundance profile of water vapour between 20 km and 60 km from our observed spectral line.

2.2. The microwave radiometer AMSOS at the ISSJ

The Airborne Millimetre and Submillimetre Wave Observing System (AMSOS) was operated in the winter months 1999 to 2001 on the ISSJ while not being used for flight campaigns, wherefore it was initially designed (Siegenthaler et al., 2001). The instrument measures the $3_{1,3} \rightarrow 2_{2,0}$ rotational transition of the water molecule $H_2{}^{16}O$ at 183.31009 GHz. A heterodyne receiver with an uncooled, sub-harmonically pumped

ACPD
3, 4833–4856, 2003

Schottky diode mixer converts the atmospheric signal to an intermediate frequency (IF) of 3.7 GHz. The IF signal is amplified by a low noise amplifier and a power amplifier and spectrally analysed with an acousto-optical spectrometer (AOS) with 1725 equally spaced channels over a bandwidth of 1 GHz. Each channel has a frequency resolution of 1 MHz. A Martin-Puplett interferometer suppresses the image sideband by more than 25 dB. The single sideband receiver noise is below 4100 K over the whole bandwidth. The atmospheric signal enters the instrument from a zenith angle of 50° through a Styrofoam window. The construction of the observation building does not allow observation at smaller zenith angles. The instrument is calibrated in a total power mode with two blackbodies at ambient and at liquid nitrogen temperature.

2.3. Raman lidar spectroscopy

The Raman lidar measurement of water vapour takes advantage of the spontaneous vibrational Raman scattering of an incident laser beam by atmospheric N_2 and H_2O molecules. The third harmonic of a Nd:YAG laser at 355 nm is used as excitation beam in zenith direction. The Raman shifted wavelengths are 387 nm from N_2 and 408 nm from H_2O, respectively. The water-vapour mixing ratio is calculated from these backscattered signals assuming a constant mixing ratio for N_2.

A correction term takes into account the differential extinction of the atmosphere at the water vapour (408 nm) and nitrogen (387 nm) Raman shifted wavelengths on the return path due to the total extinction coefficient. The total extinction term is the sum of the molecular extinction, the aerosol extinction and the molecular absorption and it is wavelength dependent. This optical extinction corresponds to an integrative effect over the entire range from the lidar site to the altitude of interest. An instrument-dependant calibration constant takes into account the transmitter and receiver optical efficiency and the quantum efficiency of the detectors for the two channels, the Raman backscatter cross section and the molecular mass and number density of the water vapour and nitrogen, respectively.

Because of this free calibration term in the forward model the number retrieved for

the water vapour mixing ratio is a relative value and an external calibration point must be added for an absolute calibration of the lidar measurements. In our case this fixpoint for the absolute value of the water vapour mixing ratio is given by humidity, pressure and temperature measurements performed routinely on Jungfraujoch by the Swiss Meteorological Institute (MétéoSuisse). This is explained in more details in Balin et al. (2001).

2.4. The Raman lidar setup at the ISSJ

The Raman lidar installed in the astronomical dome of the ISSJ is a multi-wavelength system built to probe the atmosphere above the Swiss Alps (Larchevêque et al., 2002). The transmitter of the system is based on a Nd:YAG laser (Spectra Physics, Infinity) with a maximum energy of 400 mJ at 1064 nm equipped with two non-linear crystals for second (532 nm) and third (355 nm) harmonic generation. The laser can be operated with repetition rates ranging from 20 to 100 Hz. Dichroïc mirrors at the laser output separate the three laser wavelengths and each beam is expanded 5 times in order to reduce the laser divergence from 0.7 to 0.14 mrad. These expanded beams are emitted to the atmosphere using 45° dielectric mirrors mounted on piezoelectric-driven stages. The typical output energy emitted into the atmosphere is 70 mJ at 355 nm, 60 mJ at 532 nm, and 45 mJ at 1064 nm. The lidar system is working on the vertical axis. The lidar emitter for the data analysed in this work was in off-axis configuration and thus the first data analysis can only be performed at an altitude higher than 250 m above the ground, an altitude where a full overlap of the laser beam into the telescope field of view is achieved. The receiver of this system is built around a Newtonian telescope with a primary mirror measuring 20 cm in diameter and a focal length of 80 cm. The elastic backscatter signals at 355 nm, 532 nm with parallel and perpendicular polarisation and 1064 nm as well as the Raman shifted signals from N_2 at 387 nm and H_2O at 408 nm (pumped at 355 nm) and N_2 at 607 nm (pumped at 532 nm) are simultaneously recorded. They are used to estimate the aerosol backscatter- and extinction-coefficients and the water vapour content. The backscattered light is collected by the

telescope and spectrally separated by a set of dichroïc mirrors and filters. Two sets of interference filters at each of the signal output are used to reduce the sky background light and suppress the residual elastically backscattered light in the Raman channels. This combination of filters acts as an equivalent narrow band filter with 0.5 nm FWHM at 408 nm and 387 nm, respectively and a rejection ratio of better than 10^{-7} between 200 nm and 1200 nm. Two head-on photomultiplier tubes (type EMI 9829 QA) are used in photon-counting mode. The acquisition unit has a maximum counting rate of 250 MHz and a sampling rate of 20 MHz was used.

3. Stratospheric variability

The $3_{1,3} \rightarrow 2_{2,0}$ microwave transmission line at 183 GHz is approximately 180 times stronger than the one often used for ground-based observations at 22 GHz. On the other hand the attenuation of the stratospheric signal (mostly by tropospheric water vapour) is very strong at this frequency. This is not significant for the aircraft measurements AMSOS was originally conceived for. On Jungfraujoch however, the remaining part of the troposphere above the observation site is most often opaque at 183 GHz, except for some dedicated days of extreme dryness as set forth in Siegenthaler et al. (2001). The atmospheric conditions allowed us to retrieve mixing ratio profiles for 22 days during the winters 1999/2000 and 2000/2001.

The retrieved volume mixing ratio profiles measured by AMSOS during the winters 1999/2000 and 2000/2001 are plotted in Fig. 1. Measurements span the months October (cycles), November (triangles), December (diamonds) and January (squares). An overview of the distribution of measurements over the two years of our sampling is given in Table 1.

We compare our measurements with a HALOE climatology taken from the database of N. Lautié (Lautié et al., 1999). This climatology consists of monthly mean profiles, calculated for latitude intervals of 10° each. The shaded areas in the background denote the minimum and maximum values measured by HALOE during the respec-

tive month in 1999 over the latitude circle from 40° N to 50° N. The respective mean value for the corresponding month is given by the dashed white line. To compare the HALOE profiles with our measurements we have convolved them with the averaging kernel function and the *a priori* profile of our retrieval algorithm. This method adapts the HALOE profiles to the lower resolution of our instrument which characterises our retrieved profiles (Rodgers, 2000).

We observe a general agreement between our measurements and the HALOE climatology within its variability for each month. At altitudes exceeding 45 km we tend to measure lower values than HALOE. This is especially true for the late winter month of January. For October no such statement is possible since the single retrieved profile for this month does not reach up above 45 km of altitude due to a worse signal to noise ratio in the measured spectrum corresponding to this profile. As a result of this we get a somewhat lower peak value for water vapour of 45 km to 40 km than HALOE, whose profiles normally peak at 50 km.

We explain this by the fact that in contrast to our soundings at 47° N/7° E, the HALOE climatology of latitudes between 40° N and 50° N and all longitudes includes a overly proportional contribution of measurements to the south of our observation site where water vapour is supposed to peak at higher altitude. This is because the altitude distribution of stratospheric water vapour is influenced by a down-welling over the winter pole due to the cold temperatures in the polar vortex. As a consequence, this leads to a downward movement of the water vapour peak over the polar region in northern hemisphere winter, i.e. the period of our observations.

This behaviour has been shown e.g. by Feist et al. (2003) during aircraft campaigns with the AMSOS radiometer. They have observed a transition of the peak altitude of water vapour at 47° N from about 50 km in August to about 40 km in February on two campaigns in 1998 and 1999. Our own values for the peak altitude of water vapour at this latitude, situated at 45 km to 40 km in the timespan from November to January, fit well into this evolution pattern.

Another feature we observe is that the AMSOS monthly mean mixing ratio profiles

gradually decrease as winter advances. The mean AMSOS profile for November is higher than the climatological HALOE mean profile for November, with exception of altitudes above 45 km (see Fig. 1). The latter is due to the downward propagation of the peak altitude as explained above. For December the mean AMSOS profile and the climatological HALOE mean show the same values, whereas for January the mean AMSOS profile lies below the climatological HALOE mean profile. An overview on this development is shown in detail in Fig. 2. The mean AMSOS October profile is given too in this figure, but it has to be noted that as opposed to the other months this consists of a single measurement only. Nevertheless we seem to observe the downward propagation of the water vapour peak altitude in the evolution from the October profile to the November profile. In the following months of December and January the peak altitude is at a constant 42.5 km.

4. Tropospheric variability

In contrast to the stratified stratosphere the troposphere is governed by convection and turbulence. As a result of this water vapour, like other species in the troposphere, is more variable both in time as well as in space in this altitude layer. Dynamics-related patterns, like e.g. the observed alteration of the peak altitude in stratospheric water vapour, are not perceivable in the troposphere. On the other hand we expect a higher water vapour column in summertime, where the tropopause is generally located at higher altitudes than in winter. The troposphere is also warmer in summertime due to the increased solar irradiation, which subsequentially strengthens convective forcing, leading to more thorough mixing of the troposphere. Therefore we expect a stronger variability of water vapour in summertime.

All these features can be observed in the measurements of the hygristor radiosonde and also in the lidar measurements (Fig. 3). The radiosonde, being an operational experiment, has a full coverage of the year, whereas the lidar or the microwave radiometer only perform occasional soundings. The lidar total integrated water vapour

column above the site (e.g. 4000 m a.s.l.) and the integrated radiosonde column for the same altitude range are in good correlation. The remaining differences can be explain by:

a) The natural influence of the alpine environment (mountain proximity, north-south air mass transfer above the lidar station, convective air masses guided by a rapid uplift rising from the valleys along the mountain flanks, etc.) while the radiosonde is launched from a free topography site (Payerne in the Swiss plateau).

b) The lidar profiles are generally integrated over 1–2 h, while the radiosonde is sampling the whole free troposphere in about 15–30 min.

c) The calibration value is chosen as the value measured by MétéoSuisse at the Scientific Station Jungfraujoch (e.g. 100–300 m below the first lidar point), and can make a difference in cases of high vertical variability of water vapour, which is not the case for homogeneous layers.

d) The lowest observation altitude of the lidar at 3750 m a.s.l. is slightly higher than the bottom altitude of the radiosonde water vapour column which corresponds to ∼ 3600 m a.s.l. This contribution has to be added to the lidar profile and can vary from some percents in a dry winter situation up to 20% for a high humidity summer situation.

e) Due to the high variability of the water distribution the standard deviation can reach up to 30% of the total column.

It is interesting to note that for a few days in winter the water vapour column measured by lidar yields very low values, comparable in order of magnitude to the microwave measurements for 20 km–60 km. One such occasion is the 15 January, the day for which we derive a combined profile from simultaneous microwave and lidar measurements. On this day the integrated precipitable water vapour from lidar measurements is as low as 0.24 mm (3750 m–5500 m a.s.l.), whereas the microwave radiometer measures 0.39 mm (20 km–60 km). When comparing these values we must of course not forget that the dryer the free troposphere over the Jungfraujoch is, the

shorter the column of air from which the lidar get backscatter signals becomes. It is therefore not correct to conclude from these numbers that for this day there was more water in the stratosphere than there was in the whole troposphere above 3,500 m a.s.l.

Nevertheless we find that there are a handful of days during the winter months where the atmosphere over the Jungfraujoch is indeed exceptionally dry. While this fact allows the microwave retrieval of water vapour at 183 GHz in the first place, it is also a limiting factor when attempting to combine microwave and lidar measurements to a combined profile over the whole troposphere-stratosphere as set forth in Sect. 5.

5. A combined profile

Of the 22 days where the microwave radiometer could retrieve mixing ratio profiles there was one night where the lidar has been measuring simultaneously, namely the night of 15 January 2001 from 23:30 to 00:30 UT. The microwave radiometer can only retrieve vertical distribution profiles at 183 GHz when the troposphere is extremely dry. The troposphere over the Jungfraujoch was indeed particularly dry on 15 January 2001 as can be seen in the lidar profile in Fig. 4. The Raman lidar on the other hand is dependant on a high density of molecules to provide a Raman-backscatter signal of sufficient intensity. The demands of both measuring techniques on the atmospheric condition are therefore of opposing nature. Because of the unusually dry atmospheric condition of 15 January, the Raman lidar has no signal above the noise-level for altitudes above 5.5 km as seen in Fig. 4.

The microwave radiometer derives altitude information about a species' abundance from the pressure broadening of the emission line. The upper limit to where altitude information can still be gained is given by the decreasing importance of pressure broadening at high altitudes, where the air becomes ever less dense. The lower limit is given by the observation bandwidth of the spectrometer, which cannot resolve the broad tropospheric contributions to the spectral line anymore. AMSOS can retrieve a vertical distribution of the water vapour mixing ratio with less than 20% *a priori* contribution

between 20 km and 60 km a.s.l.

The upper limit of the lidar profile is given by the intensity of the received Raman backscatter signal. This is basically a function of the number of scattering particles but also the dimensions of the detecting optical telescope. On the exceptionally dry day considered in this study the Raman lidar on Jungfraujoch can retrieve a water vapour mixing ratio profile up to 5.5 km a.s.l. When trying to combine the two datasets we therefore face a gap in altitude from 5.5 km to 15 km where we have no measurements from either the microwave radiometer or the lidar.

Potential alternative measurement techniques to be considered for closing the altitude gap between the lidar measurements and the microwave measurements are the radiosondes of MétéoSuisse or satellites. One operational radiosonde was launched at Payerne (85 km to the west-northwest of Jungfraujoch) at the same time as the lidar sampling. Figure 4 shows that there is a big discrepancy between the radiosonde at Payerne and the lidar on the Jungfraujoch which is probably due to the high variability of tropospheric water vapour both in space and time. Also the radiosonde profile can only be trusted up to ∼6.5 km, where the temperature on this day falls below −37°C. The reason for this is that carbon hygristors are known to loose their responsiveness below temperatures of −35°C to −40°C, depending on their manufacturing (Jeannet et al., 2001). A new experimental sensor by the name of SnowWhite, featuring a chilled mirror dew-point hygrometer, is occasionally launched by MétéoSuisse. The SnowWhite sounding closest to our observation in time was performed on 17 January 2003. This sounding delivers a reliable water vapour profile up to an altitude of ∼10.5 km (Jeannet and Levrat, 2003). Unfortunately, given the large variability of water vapour in the troposphere, the results of said SnowWhite sounding does not capture the conditions we had during our combined measurement on 15 January and therefore it is even less suitable than the simultaneously launched operational sonde to directly fill the gap between our measurements. Satellite measurements are not suitable either because mostly they do not reach down to the tropopause and never have enough spatial resolution that a comparison with our profile above a strictly confined location would make

ACPD
3, 4833–4856, 2003

sense.

We suggest the following approach to use the microwave *a priori* profile to bridge the altitude gap down to the lidar measurements. The retrieval algorithm of the microwave radiometer will generally produce a compromise solution between an *a priori* profile and a measurement. On altitude levels where the information content of the measurement is high the retrieved profile will feature the true atmospheric distribution. However on altitude levels too high or low for the radiometer to resolve the retrieved profile will basically reflect the *a priori* profile. This process is a gradual one. For AMSOS the *a priori* contribution to the retrieved profile grows above 20% at altitudes below 20 km and above 60 km. There we would normally cut off our retrieved profile because the values we get are *a priori* values and do not reflect the state of the atmosphere during the measurement.

With the lidar measurement in the troposphere on the other hand we have a clear knowledge about the water vapour distribution from our observation site up to 5.5 km. When we scale the tropospheric part of our *a priori* profile to match the lidar data we have an *a priori* profile which reflects the true state of the troposphere the moment of the microwave sounding. The tropopause has been chosen as the upper limit to where the initial *a priori* profile is scaled to overlap the lidar measurements. This validated *a priori* profile is subsequentially being used to retrieve stratospheric water vapour. The benefits from this method are twofold:

First off all we increase the accuracy of our retrieval because we have a very exact model of the troposphere. Tropospheric attenuation has to be considered in the radiative transfer when retrieving microwave spectra.

Secondly we do not have to cut off the parts below 20 km of our retrieved profile because of the substantial *a priori* contribution anymore. While the *a priori* contribution will of course still be significant at these altitudes, we do know from the initial *a priori* generation that the tropospheric part of the *a priori* reflects the true state of the atmosphere known from lidar measurement.

The profile we gained this way is shown in Fig. 5. In this figure the solid black line

depicts the combined microwave-lidar profile and the dotted black line the microwave *a priori* profile. Numeric values for the combined microwave-lidar profile and errors are given in Table 2.

The microwave part is merging smoothly into the lidar part in the region of the tropopause, where the microwave profile changes from information on the state of the atmosphere to *a priori* information (which is equal per definition to the lidar measurement). It has to be noted that the profile in Fig. 5 is of higher resolution in the troposphere than in the stratosphere. The microwave retrieval per se will of course conserve its lower resolution also in the troposphere. Therefore the profile in Fig. 5 is a combination of the microwave data above the tropopause and the lidar data below the tropopause. The joint of the two profiles at the tropopause is canonically a smooth one. This follows directly from the method by which the microwave *a priori* profile has been chosen.

The error-bars denote the retrieval errors of the microwave and lidar retrieval, the former for the stratosphere and the latter for the troposphere, respectively. In the intermediate section, where the combined profile follows the lidar-bound *a priori* profile, the mixing ratio values can not directly be attributed to an instrument measurement. For this region we use the interpolated relative error between the topmost lidar measurement and the bottommost microwave measurement as the overall error estimate. Error-bars derived this way are denoted by a $\star$ in Table 2. We hereby achieve a smooth evolution of the errors over the tropopause region while respecting the magnitude of errors at altitudes where error calculations from data retrieval exist.

In the background we plotted the climatological mean HALOE profile of January together with its minimum and maximum values.

6. Conclusions

The atmospheric water vapour distribution has been measured from the International Scientific Station Jungfraujoch in the Swiss Alps in the winters 1999/2000 and

2000/2001. A microwave radiometer measuring at 183 GHz retrieves stratospheric profiles from 20 km up to 60 km of altitude, while a Raman lidar retrieves profiles for the free troposphere from the observation altitude of 3500 m a.s.l. up to about 10 km. The microwave emission line is only visible on very dry tropospheric conditions with tropospheric transmittances of 0.3 or higher at our observation angle of 50° (Siegenthaler et al., 2001). For the period observed the microwave radiometer could retrieve 22 volume mixing ratio profiles spread over the months of October to January. These profiles have been compared to a HALOE monthly climatology for the zonal girdle between 40° N and 50° N. Our measurements are in good agreement with the HALOE climatology within its monthly variability. We observe a lower water vapour peak altitude than HALOE, a fact that we relate to the more numerous presence of HALOE measurements to the south of our observation latitude than of those to the north. In the winter months the water vapour peak shows a downward gradient towards the pole because of the downwelling of air in the polar vortex. Judging from our monthly mean profiles this downward propagation of the peak altitude seems to happen between October and November. We further observe a continuous decrease in water vapour mixing ratios throughout the months of November to January in our monthly mean profiles.

The variability of the integrated precipitable water vapour column above Jungfraujoch was determined from Raman lidar measurements. The data show increased humidity and larger variations in summer, which is in accordance with data from a hygristor radiosonde by MétéoSuisse. On some days in the winter the water vapour column measured by lidar for the few kilometres above Jungfraujoch can reach values down to the order of what the microwave radiometer measures for the whole stratosphere. One such day was 15 January, on which the simultaneous microwave – lidar observation took place.

In spite of the opposing requirements on atmospheric conditions of the two instruments and the non-continuous sampling rate we have one hour of simultaneous observation by the microwave radiometer and the lidar on 15 January 2001 from 23:30 to 00:30 UT. Lidar measurements only reach up to 6 km on this day because of the ex-

tremely dry troposphere. The dryness of the troposphere above Jungfraujoch shows up in comparison with a radiosonde profile launched at the same time in Payerne, 85 km to the west-norhtwest of the Jungfraujoch. The radiosonde does not reach above the observation altitude of the lidar because the carbon hygristor becomes inaccurate at temperatures close to and below $\sim -40^{\circ}$C which were measured at this altitude. A frost point hygrometer launched about two days later also at Payerne delivers a water vapour profile up to an altitude of ~10.5 km, but because of the difference in time and place it does not represent the dry air we measured the night of our simultaneous observations.

We suggest the following method to combine the two measurements and to bridge the altitude gap where no direct measurements exist. We adapt the *a priori* profile used in the microwave retrieval to match the tropospheric water vapour distribution measured by the lidar and then subsequently use this validated *a priori* information to retrieve the microwave profile. This extends the validity range our microwave profile, which will consist mainly of *a priori* information below about 20 km, down to the troposphere. Even though the retrieval altitudes below 20 km consist largely of *a priori* information, this will not corrupt the accuracy of our retrieved profile since we know from the lidar sounding that the *a priori* profile reflects the true state of the troposphere. We hereby get an exemplary water vapour profile for a dry winter atmosphere from 3500 m a.s.l. up to 60 km. This is the first time to the knowledge of the authors that microwave and lidar soundings have been performed simultaneously and from the same location in order to obtain a vertical water vapour distribution profile of the whole free troposphere and stratosphere together. Even though there remains an altitude gap with no direct measurements when combining the two techniques, we believe that the method presented to bridge this gap yields a more realistic profile than simple interpolation would produce. In making use of *a priori* information we increase the information content of the intermediate section in comparision to a purely mathematical interpolation approach.

Acknowledgements. We thank P. Jeannet from MétéoSuisse for providing us with profiles of the SnowWhite sonde. We thank MétéoSuisse for providing us with the hygristor data from their

regular radiosondes from Payerne. Special thanks go to the International Scientific Station Jungfraujoch, which allows us to use their facility for our research.

References

Balin, I., Larchevêque, G., Quaglia, P., Simeonov, V., van den Bergh, H., and Calpini, B.,: Water vapor vertical profile by raman lidar in the free troposphere from the jungfraujoch alpine station, in Press in ADVANCES IN GLOBAL CHANGE RESEARCH, vol. 9, Kluwer Academic Publishers, 2001. 4837

England, M. N., Ferrare, R. A., Melfi, S. H., Whiteman, D. N., and Clark, T. A.: Atmospheric water vapour measurements: Comparison of microwave radiometry and lidar, JGREA, 97, 899–916, 1992. 4834

Feist, D., Vasic, V.; and Kämpfer, N.: Aircraft measurements of the variability of stratospheric water vapor over the norhtern hemisphere, Poster at the 83rd annual Metting of the American Meteorological Society, Long Beach CA, 2003. 4839

Jeannet, P. and Levrat, G.: Mesures des profiles d'humidité du 17.01.2001 avec hygromètre à miroir SnowWhite et hygristor VIZ: Note à l'attention de M. D. Gerber, Personal Communication, 2003. 4843

Jeannet, P., Ruppert, P., Hoegger, B., and Levrat, G.: Atmosphärische Wasserdampfprofile mittels Taupunktspiegel–Hygrometer, DACH–MT 2001, Wien, 18–21 Sept. 2001, 2001. 4843

Kley, D., Russell III, J. M., and Phillips, C. (eds.): SPARC assessment of upper tropospheric and stratospheric water vapour, no. WCRP-113 in World Climate Research Programme Reports, SPARC Office, BP 3, 91371 Verrières le Buisson Cedex, France, 2000. 4834

Larchevêque, G., Balin, I., Nessler, R., Quaglia, P., Simeonov, V., van den Bergh, H., and Calpini, B.: Development of a multiwavelength aerosol and water–vapour lidar at the jungfraujoch alpine station (3580 m above sea level) in switzerland, APOPA, 41, 2781–2790, 2002. 4837

Lautié, N., de la Nöe, J., and Ricaud, P.: A water vapour profiles database, in Fith European Workshop on Stratospheric Ozone, 1999. 4838

Nedoluha, G. E., Bevilacqua, R. M., Gomez, R. M., Siskind, D. E., Hicks, B. C., Russell III, J. M., and Connor, B. J.: Increases in middle atmospheric water vapor as observed by the Halogen

Occultation Experiment and the ground-based Water Vapor Millimeter-wave Spectrometer from 1991 to 1997, Journal of Geophysical Research, 103, 3531–3543, 1998. 4834

Rodgers, C. D.: Inverse Methods for Atmospheric Sounding: Theory and Practise, vol. 2 of Series on atmospheric, oceanic and planetary physics, World Scientific Publishing Co.Pte.Ltd., P O Box 128, Farrer Road, Singapore 912805, ISBN 981-02-2740-X, 2000. 4835, 4839

Siegenthaler, A., Lezeaux, O., Feist, D. G., and Kämpfer, N.: First water vapor measurements at 183 GHz from the high alpine station Jungfraujoch, IEEE Transactions on Geoscience and Remote Sensing, 39, 2084–2086, 2001. 4835, 4838, 4846

Starr, D. O. and Melfie, S. H. (eds.): The Role of Water–vapor in Climate: A Strategic Research Plan for the Proposed GEWEX, Water Vapor Project (GVaP), vol. CP–3120 of NASA Conf. Proc., 1991. 4834

Table 1. Distribution of AMSOS samplings for which mixing ratio profiles could be retrieved during the winters 1999/2000 and 2000/2001

Number of samplings	1999/2000	2000/2001	Overall
Oct	–	1	1
Nov	4	–	4
Dec	4	2	6
Jan	7	4	11
Overall	17	7	22

ACPD
3, 4833–4856, 2003

Table 2. Numeric values of the combined microwave-lidar profile of 15 January 2001. Errorbars denote retrieval errors of the lidar (troposphere) and the microwave radiometer (stratosphere), respectively. Values with a ⋆ are interpolated relative errors

Alt. (km)	Mix. Ratio (ppmv)	Error (ppmv)	Alt. (km)	Mix. Ratio (ppmv)	Error (ppmv)
4.0	385.12	53.17	12.5	3.44	⋆ 1.07
4.5	254.00	67.67	17.5	4.06	0.72
5.0	110.38	45.11	22.5	4.47	0.40
5.5	62.88	45.11	27.5	4.91	0.48
6.0	47.29	33.83	32.5	5.31	0.52
6.5	35.21	⋆ 24.09	37.5	5.81	0.61
7.0	28.82	⋆ 18.83	42.5	6.20	0.70
7.5	23.62	⋆ 14.70	47.5	5.62	0.80
8.0	18.89	⋆ 11.17	52.5	4.65	0.78
8.5	13.42	⋆ 7.52	57.5	3.75	0.90
9.0	10.58	⋆ 5.60	62.5	3.29	1.01
9.5	7.29	⋆ 3.63	67.5	3.04	0.78
10.0	5.48	⋆ 2.56	72.5	2.42	0.38
10.5	5.15	⋆ 2.24	77.5	1.92	0.15
11.0	4.78	⋆ 1.94	82.5	1.96	0.07
11.5	4.38	⋆ 1.64	87.5	2.50	0.04
12.0	3.93	⋆ 1.35			

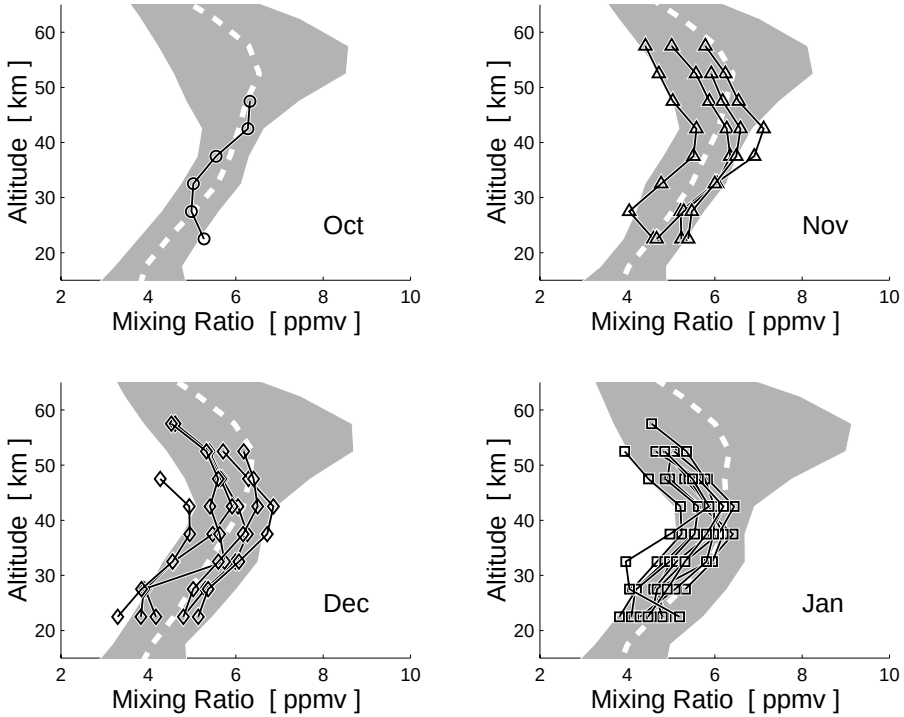

Fig. 1. Stratospheric water vapour distribution over the Jungfraujoch measured by microwave radiometry for the winters 1999/2000 and 2000/2001. The profiles are plotted by month. The shaded areas in the background are the minimal and maximal values of the 1999 HALOE monthly mean for the corresponding month. The dashed white lines are the respective HALOE monthly mean profiles.

ACPD
3, 4833–4856, 2003

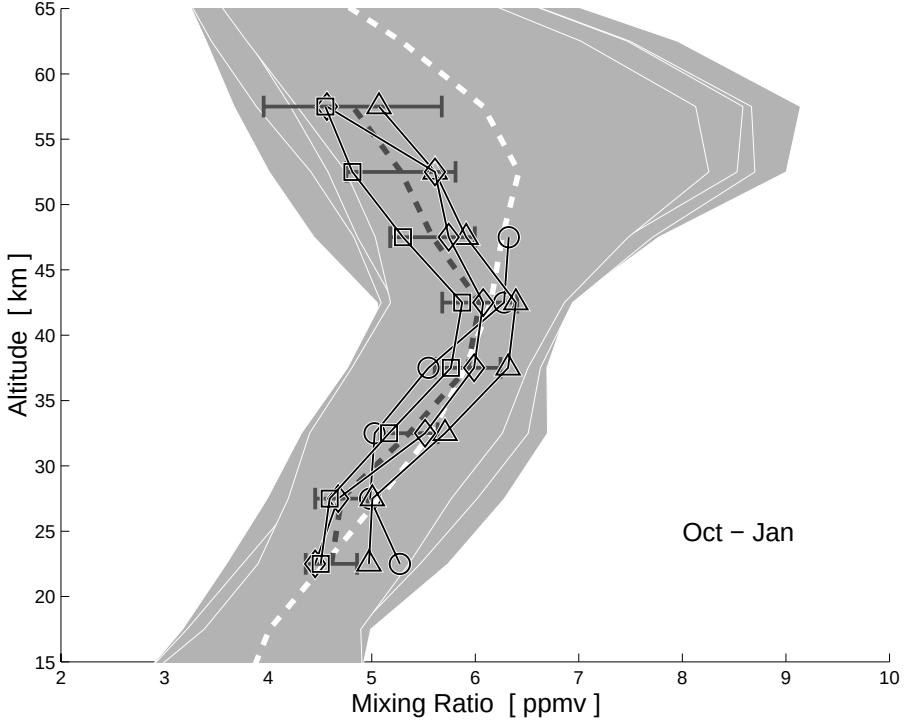

Fig. 2. Stratospheric water vapour distribution over the Jungfraujoch measured by microwave radiometry for the winters 1999 to 2001. The profiles are monthly means from October (circles), November (triangles), December (diamonds) and January (squares), respectively. The shaded areas in the background (distinguished by their white borders) are the minimal and maximal values of the HALOE monthly and zonal mean for the months October to January 1999. The dashed white line is the HALOE monthly mean profile for these four months. The dashed gray line with error-bars is the AMSOS mean profile for all four months October to January 1999 to 2001.

ACPD
3, 4833–4856, 2003

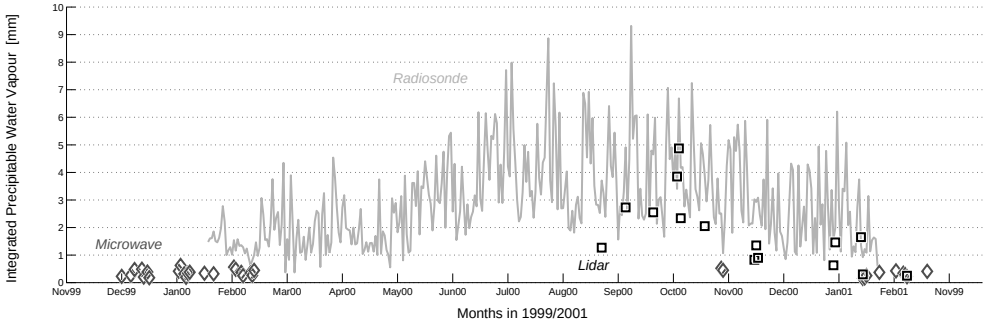

Fig. 3. Integrated precipitable water vapour in [mm] measured by radiosonde from Payerne (light gray) and by Raman lidar (black squares) and microwave radiometer (gray diamonds) from Jungfraujoch. The radiosonde measurements span the free troposphere from 3600 m a.s.l. up to the sounding limit of the balloon. Lidar measurements are from 3750 m a.s.l. up to the detection limit. The microwave measurements represent the stratosphere from 20 km to 60 km.

ACPD
3, 4833–4856, 2003

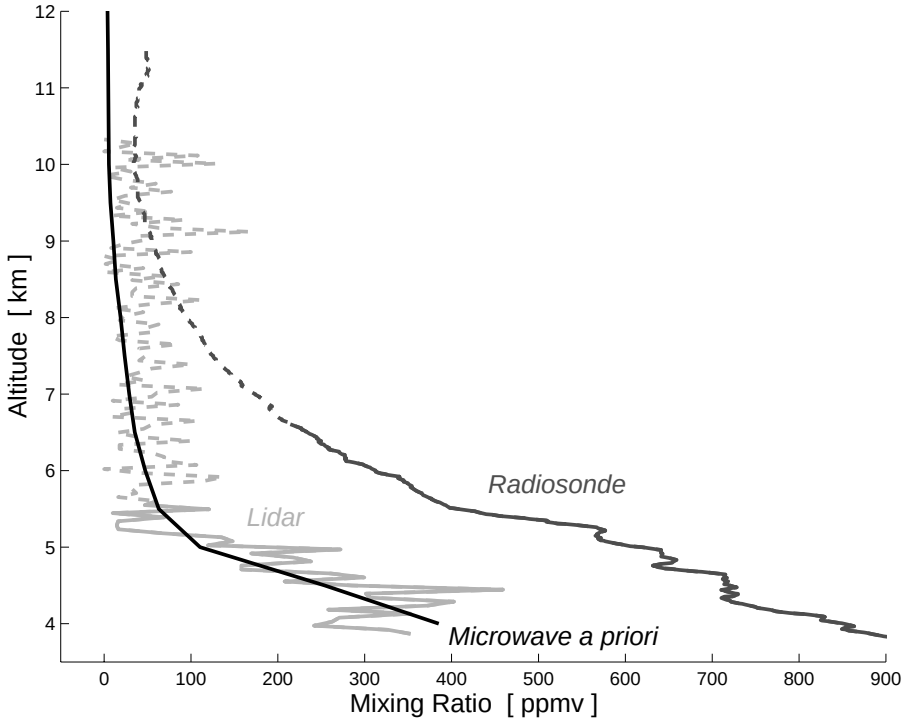

Fig. 4. Tropospheric profiles of the Raman lidar (light gray) and the Payerne radiosonde (dark gray). The dashed part of the lidar profile is where the signal to noise ratio falls beyond the detection threshold. The dashed part of the radiosonde profile denotes temperatures below −37° Celsius, at which the response of the carbon hygristor degrades. The black line is the microwave *a priori* profile tied to the lidar measurements at altitudes where the latter is valid. This is identical to the combined microwave-lidar profile at the altitudes shown here.

ACPD
3, 4833–4856, 2003

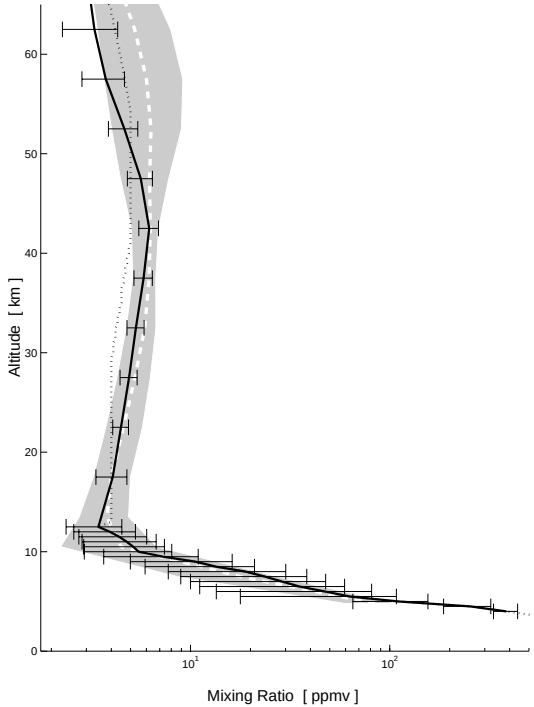

Fig. 5. Combined microwave-lidar profile (black line) of 15 January 2001 for both the troposphere and stratosphere. The dotted black line is the *a priori* profile of the microwave retrieval. The tropospheric part of the *a priori* is given by the lidar measurement. Below the tropopause at 12.5 km the combined profile is identical to the *a priori*. The shaded area in the background is the minimal and maximal value of the HALOE monthly and zonal mean for the month of January. The dashed white line is the HALOE monthly mean profile for this month. The abscissa is in logarithmic scale to account for the large difference in abundance over the altitudes considered.

ACPD
3, 4833–4856, 2003